

Reliability of micro/macro- fatigue crack growth behavior in the wires of cable-stayed bridge

Keke Tang^{1,2,*}

¹ Key Laboratory of Pressure Systems and Safety, Ministry of Education, School of Mechanical Engineering and Power Equipment, East China University of Science and Technology, Shanghai 200237, China

² Department of Engineering Mechanics, Southeast University, No.2 Si Pai Lou, Nanjing 210096, China

* Corresponding author: kktang@ecust.edu.cn

Abstract

The principle of least variance is applied to evaluate the reliability of fatigue crack growth behavior in the steel wires of Runyang cable-stayed bridge. Micro/macro- crack growth model is proposed in that both micro- and macro scale effects can be included. These features are best exhibited by the normalized generic parameters that reflect the effects of material, loading and geometry. Attention is paid to the 5mm diameter wire in cables under traffic that is reflected by the additional applied tension force. Combination of theory of least variance and the dual scale model offers a new perspective for the reliability analyses of structural systems. The aim is to demonstrate there exists a time range of high reliability for the crack length history that correspond to the least variance of the time dependent R-integrals. The results coincide with the scale range established empirically by in-service health monitoring for micro-macro cracking. Such agreements are encouraging with regard to the potential application of principle of least variance in multiscale reliability assessment for multi-component and multi-function systems.

Keywords Reliability, Least variance, Micro/macro- crack growth model, Cable-stayed bridge, Fatigue

1. Introduction

Bridges, particularly cable-stayed bridges, are the superstar of engineering world. Aesthetically, they allow for creative freedom by varying the shape of towers and arrangement of the cables. Technically speaking, the critical components in a cable-stayed bridge are clearly the cables that behave differently and act as a structure in itself. Each of the cables consists of bundles of high strength steel wires. The structural integrity is inevitably affected by the degradation of the individual cables and wires, making replacement of cables necessary and crucial events during the life span of cable-stayed bridges. For this reason alone, rational assessment of the reliability of in-service cables in structural health monitoring can be of a big concern. However, multiple factors such as material degradation, changing environment and operating conditions, in many cases, have made structural reliability hard to predict.

Fatigue crack growth behavior in wires of cables plays a substantial role in the degradation of the individual wires and cables, which stands out in the reliability analyses. Specifically for the 5mm diameter steel wires included in cables, the crack initiation and propagation are intimately related under traffic load, such that they should be treated as the same process. Fatigue damage accumulation occurs at distinctive scales. The conventional crack growth approach [1] is no longer applicable and a dual scale crack growth model in which both micro- and macro- effects are involved, should be mandated. Demonstrated in [2] are earlier researches on dual scaling. Studied in [3] was the loosening and tightening effects on the fatigue crack growth behavior of cables and wires for the cable-stayed portion of Runyang Bridge. However, emphasized here are the reliability analyses of fatigue crack growth behavior in wires. In spite of unpredictable difficulties, it is, however, desirable to let the service time span be coincident with the reliable portion. The attainment of such a goal is not straightforward because of the interactive effects of material, load and geometry. They can compensate the trade off with one another. Their delineation has been problematic. Recent works on the principle of least variance [4, 5] has shown that ‘trade-off effect’ can be made more transparent by exploring the variables including length [6-8], velocity, mass and

energy. Under extreme conditions they are expressed as large versus small; fast versus slow; thick versus thin; high versus low. The extreme conditions are those that deviate more appreciably from the mean or the average. They are regarded as being ‘least’ reliable, while the opposite being ‘most’ reliable.

Application of the least variance approach will be made to investigate the reliability aspects of the fatigue crack growth behavior in the wires of Runyang cable-stayed bridge. Dual scale fatigue crack growth model is employed. Only cable that undergoes the most severe tension under traffic will be singled out to be explored for the purpose of reliability analyses.

2. Problem statement of cable-stayed portion of Runyang bridge

The Runyang Bridge [9] consists of two major bridges that link the south bank and the north bank. The south bridge is a suspension bridge with a main span of 1,490 meters. The north bridge is a cable-stayed bridge with a main span of 406 meters. Keep in mind that current research is focused on the cable-stayed portion, compare Fig.1. The cables are mounted onto the two towers and anchored at the girders of the bridge. Due to the load variations, tightening and loosening of the cables is expected. Only tightening case for reliability analyses will be discussed in the current work.

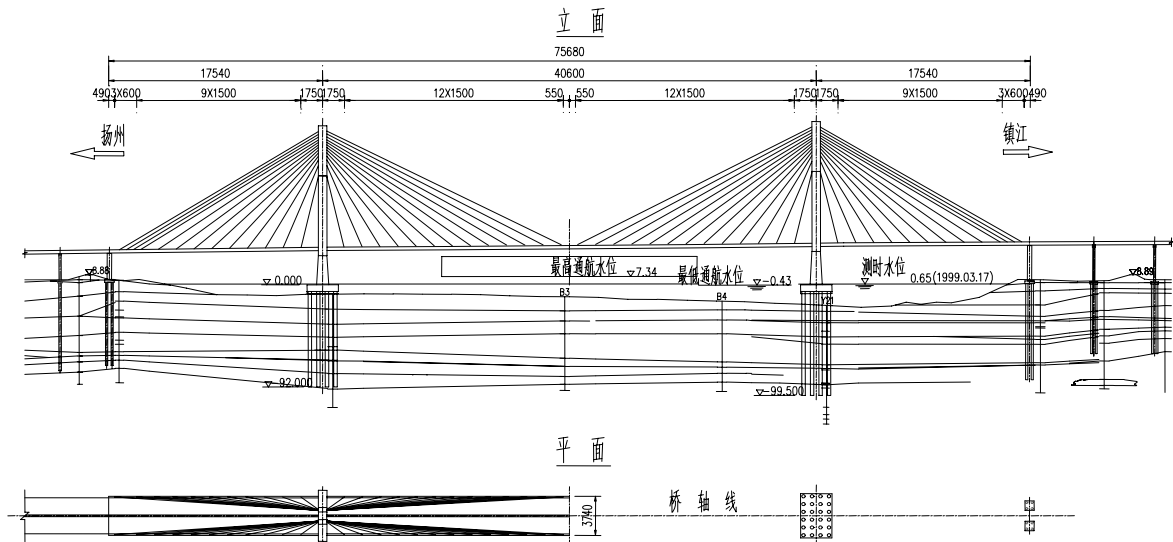


Fig.1 Cable-stayed portion of Runyang Bridge

2.1. Cable forces with and without traffic

There are 104 cables used to support the deck with the help of towers. Due to the symmetry, only a total of 52 cables on each side need to be shown here. The position of each cable is shown and numbered from left to right in Fig.2. Note the largest forces prevail in cable no.3 and no.50. Therefore only cable no.3 will be chosen to demonstrate the reliability of fatigue crack growth behavior.

A detailed description of cable construction can be referred to Fig.3. The cable consists of multiple high strength steel strands arranged in a bundle and encased in a polyethylene pipe filled with cement grout. Since the polymer carries little load and their resistance can be neglected. Each cable consists of 37 stranded steel ropes and each of the ropes contains 7 galvanized steel wires. Hence, a total of 259 galvanized steel wires construct one cable. With the diameter of steel wire being 5mm, the stress calculation thus is executed based on the effective section areas as follows

$$\sigma = \frac{F}{A_c} \quad (1)$$

in which F is the cable force and A_c being the effective cross section of each cable.

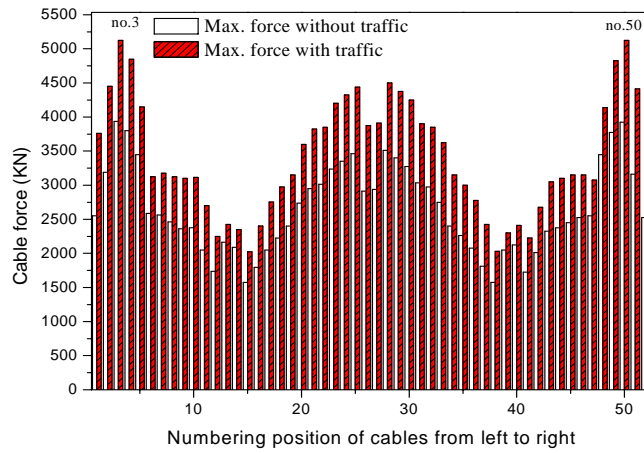


Fig.2 Maximum and minimum loads in cables with/without traffic

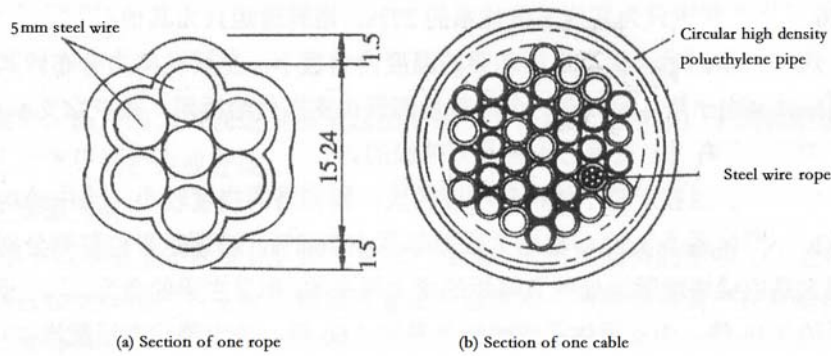


Fig.3 A typical section of the bridge cable

2.2. Tightening and loosening of cables and wires

Variations of the tension in the cable and wire, a set of $\sigma_a \sigma_m$ for the cable and wire will be defined. They are referred to be Cases I and II.

$$\text{Case I} \quad \sigma_a = \eta \sigma_{\max}^\eta - \sigma_{\max}^0, \quad \sigma_m = \frac{\eta \sigma_{\max}^\eta + \sigma_{\max}^0}{2} \quad (2)$$

$$\text{Case II} \quad \sigma_a = \sigma_{\max}^\eta - \eta \sigma_{\max}^0, \quad \sigma_m = \frac{\sigma_{\max}^\eta + \eta \sigma_{\max}^0}{2} \quad (3)$$

σ_a and σ_m respectively denote stress amplitude and mean stress. σ_{\max}^η and σ_{\max}^0 in Eqs. (2) and (3) represent the maximum stress with and without traffic. Note the parameter α greater than 1 reflect the degree of cable tightening, while η less than 1 reflect the degree of cable loosening. Bear in mind that $\eta = 1.0$ stands for normal tension. Fig. 4 displays a plot of the product $\sigma_a \sigma_m$ for the cables as a function of the cable position from left to right numbered as 1 to 52. The product

$\sigma_a \sigma_m$ fluctuates according to the variations of the tension in the cables with traffic load. Notice the peaks of the curves correspond to cable no.3 and no.50 in which maximum cable forces occur.

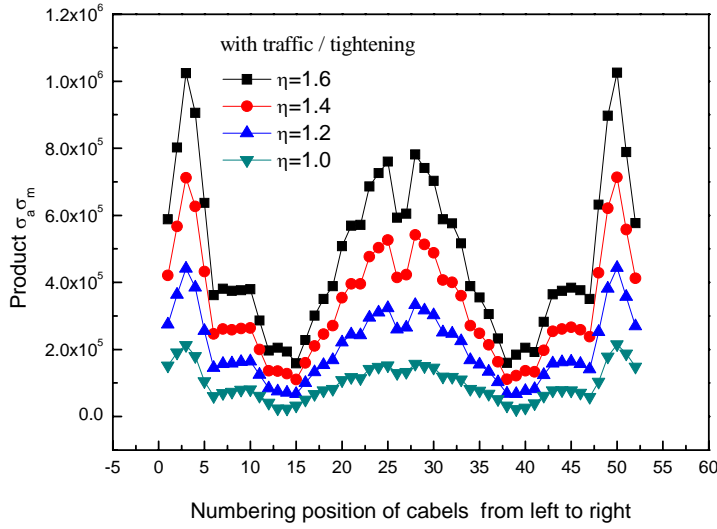


Fig.4 Product $\sigma_a \sigma_m$ of cables versus position of cables for tightening case under varying traffic

3. Multiscale micro/macro- fatigue crack growth model

3.1. Fatigue crack growth of steel wire

There are three normalized physical parameters σ^* ($=\sigma_0/\sigma_\infty$), μ^* ($=\mu_{\text{micro}}/\mu_{\text{macro}}$) and d^* ($=d/d_0$) defined in the micro/macro- fatigue crack growth model. They, respectively, reflect the influences of load, material and geometry.

$$\mu^* = \frac{\mu_{\text{micro}}}{\mu_{\text{macro}}}, \quad d^* = \frac{d}{d_0}, \quad \sigma^* = \frac{\sigma_0}{\sigma_\infty} \quad (4)$$

When it comes to structural applications, incidental material parameters can be absorbed by the macro empirical parameters which will be confined to two. Thus further being incorporated into the current fracture control approach expressed as follows:

$$\frac{da}{dN} = B(\Delta S_{\text{micro}}^{\text{macro}})^m \quad (5)$$

where floating parameters B and m can be found by test data in a regular fatigue test. Here, B is the y-intercept and m being the slope of the curve for the straight line portion of the log-log plot of Eq. (5). The crack length can be computed by integrating Eq. (5). $\Delta S_{\text{micro}}^{\text{macro}}$ has the following expression:

$$\Delta S_{\text{micro}}^{\text{macro}} = \frac{2(1-2\nu_{\text{micro}})(1-\nu_{\text{macro}})^2 \sigma_a \sigma_m a}{\mu_{\text{macro}}} \mu^* \sqrt{d^*} \sqrt{\frac{d_0}{r}} (1-\sigma^*)^2 \quad (6)$$

in which σ^* is the ratio of material restraining stress σ_0 to the applied stress σ_∞ . σ^* must always be less than one. This corresponds to the threshold for the onset of crack growth. d^* is the normalized characteristic dimension compared to the microscopic length d_0 . r is the radial distance from the crack tip. μ^* is the ratio of microscopic modulus μ_{micro} to the macroscopic modulus μ_{macro} . ν_{micro} and ν_{macro} respectively stand for the Poisson's ratio at micro- and macro-scales.

3.2. Fatigue properties of steel wire

Macroscopic material properties such as steel can be achieved from experimental test. Refer to Table 1 for the mechanical properties of bridge steel wire.

Table 1. Mechanical properties of bridge steel wire [9]

| Elastic modulus E_{macro} | Shear modulus μ_{macro} | Poisson's ratio ν_{macro} |
|-----------------------------|-----------------------------|-------------------------------|
| 199.81GPa | 76.85GPa | 0.3 |

Without going into the details, the floating parameters B and m are given by [10,11]

$$m = 1, \quad B = 2.15 \times 10^{-6} \quad (7)$$

Microscopic material properties cannot be achieved through specimen test as macroscopic properties do. They prevail, more specifically, at local place comparing to the big bulk of macroscopic specimen and are location dependent. The following assumptions are made:

$$\begin{aligned} \mu^* = \frac{\mu_{micro}}{\mu_{macro}} = 2, \quad d^* = \frac{d}{d_0} = 1, \quad \sigma^* = \frac{\sigma_0}{\sigma_\infty} = 0.3, \\ d_0 = 10^{-3} \text{ mm}, \quad \nu_{micro} = 0.4, \quad \frac{d_0}{r} = 1 \end{aligned} \quad (8)$$

This completes all the parameters in the micro/macro fatigue crack growth model. Crack length and velocity history thus can be explicitly illustrated.

4. Theory of least variance for reliability

Reliability is associated with the failure of a component or system to satisfy the intended function for a specified period of time. Uncertainties can have a major effect on the cause of failure. They can be attributed to degradation of material properties, variance of loading and change of environmental conditions. These changes can affect the reliability of long run predictions. Hindsight is not a solution here. It is unrealistic to overemphasize the deterministic and probabilistic aspects of life prediction. However, there is still the need to understand the physical applications of the monitored data. Crack initiation and propagation should be treated as multiscale transition process. Time increment effects also affect reliability differently for the different scale ranges such as micro to macro scale, which can be reflected by the weighted functions proposed in the theory of least variance.

4.1. R-integrals

Let n denotes the number of R-integral R_1, R_2, \dots, R_n which correspond, respectively, to

$$\int_0^{t_1} \alpha_1(t) p_1^{a_1}(t) dt, \int_0^{t_2} \alpha_2(t) p_2^{a_2}(t) dt, \dots, \int_0^{t_n} \alpha_n(t) p_n^{a_n}(t) dt \quad (9)$$

When a^1, a^2, \dots, a^n are given, then $p_1(t), p_2(t), \dots, p_n(t)$ are treated as ordinary functions. If $a^1 = a^2 = a^3 = a^4 = 1$, then $p_1(t), p_2(t), p_3(t)$ and $p_4(t)$ stand for the four root functions defined in the CTM/IDM theory [12,13]. They correspond, respectively, to the length, velocity, mass density and energy density. The weighted functions $\alpha_1(t), \alpha_2(t), \dots, \alpha_n(t)$ interconnect the space-time effects at the different scale ranges. Depending on the number of time segments chosen by normalizing

$$p_1(t) = a_1(t) / a_1(0), \quad p_2(t) = a_2(t) / a_2(0), \quad \dots, \quad p_n(t) = a_n(t) / a_n(0) \quad (10)$$

Note that the initial values of $a_1(t), a_2(t), \dots, a_n(t)$ at $t = 0$ are given by $a_1(0), a_2(0), \dots, a_n(0)$.

4.2. Principle of least variance

As a rule, reliability counts on the continuous operation of systems in time. Since physical systems are inherently non-homogeneous, ranking the different degree of variability would be of potential solution. Identifying the least reliable space-time segment of the system operation will be made by invoking the ‘principle of least variance’ which can be stated as:

The segment with the least variance ΔR_i is assumed to be most reliable up to the time t_f of potential failure.

The variance ΔR_i is obtained by the linear sum average (LS) of the R-integrals

$$R_{ave}^{LS} = \frac{1}{n} \sum_{i=1}^n R_i \quad (11)$$

Other approaches including root mean square average (RMS) or inverse linear sum average (ILS) are also the options. However, they are outside the scope of this work.

The absolute value of the deviation of each of the R_i from the average will be referred to as the variance ΔR_i . The expression for LS variance is

$$\Delta R_i^{LS} = |R_i^{LS} - R_{ave}^{LS}| \quad (12)$$

Minimizing the oscillation of R_1, R_2, \dots, R_n with reference to their average has been assumed to be a possible measure of system reliability. The principle of least variance identifies the time span to which ΔR_i takes the smallest values. Hence, range of reliability will be decided on the basis of linear sum average.

5. Reliability of micro/macro- fatigue crack growth history in steel wire

Conventionally three regions are divided along the sigmoidal curve for the plot of $\log da/dN$ versus $\log \Delta K$. They are referred to, respectively, as crack initiation, stable crack growth and fast fracture. Crack locally initiates from a very small length and extends slowly in a relatively stable fashion. It finally enters into the stage of fast fracture. In practical engineering, non-destructive testing measurements of the crack length are made for establishing the period of maintenance before the curve turns around the corner into the region of rapid crack propagation. The point to be made here is, there exists a region where crack grows slowly and stably is most reliable for detection, refer to Fig.5 for the range of reliability in practice.

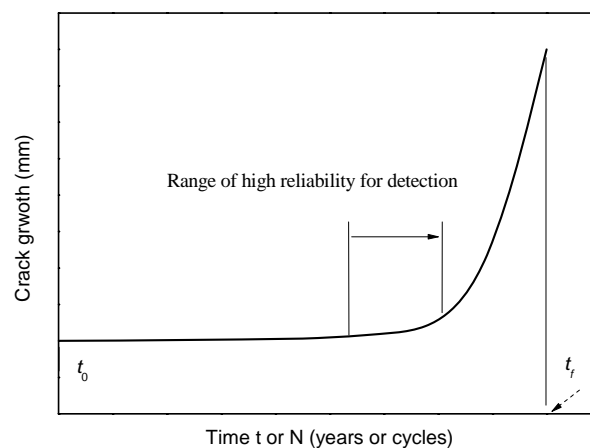


Fig. 5 Range of high reliability for fatigue crack growth

5.1. Micro/macro- fatigue crack growth in steel wire

An initial crack length of 0.2mm is taken compared to the 5mm diameter of steel wire. Keep in mind that the cables of bridges are usually replaced every 10 years. The situation also varies with the positions of the cables since they bear tremendously different cable forces under traffic. Breakage of steel wires cause the cable failure, although multiple factors such as corrosion also come into play during the operating period of bridges. Assumption of 10-year in-service of cable is made here for simplification. This gives steel wire roughly 10 years of fatigue life. Conversion of the crack length fatigue cycle history to the corresponding time history requires the specification of load frequency. The following load frequency is proposed:

$$dN / dt = 80,000 \text{ cycles / year} \quad (12)$$

Combining Eqs (7), (8) and (12), Eq. (6) can be put into Eq. (5) for finding $a(t)$ by integration from 0 to t with an initial crack length of 0.2mm. Depicted in Fig. 6 is the graphical presentation of crack length growth history of steel wires in cables. Recall only cable no.3 is selected since it bears the biggest cable force among 52 cables listed.

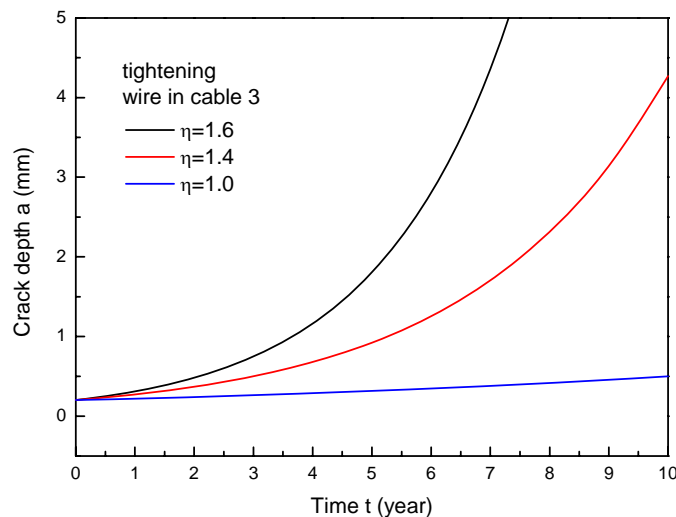


Fig.6 Crack depth a versus time t (years) for cable no.3 with tightening effects under traffic

The reference crack growth curve is given by $\eta = 1.0$ as shown in the bottom of Fig.6. It remained nearly constant for the range of 10 years. As the cable is tightened gradually with the perturbation parameter $\eta = 1.4$ and 1.6 . The curves deviate from the reference with increasing crack length. The crack depth reaches 5mm approximately at 7 years for tightening coefficient $\eta = 1.6$. Even for $\eta = 1.4$, the crack depth is over 4mm after 10 years. Thus conclusion can be made that increase of cable tension tends to enhance crack growth.

5.2. Reliability of micro/macro fatigue crack growth history of steel wires

The reliability of fatigue crack growth vary during the life span. Determination of the reliable portion of fatigue crack growth will be studied by applying the principle of least variance. This will be done based on the crack growth history obtained in Fig.6.

5.2.1. Weighted functions

Notice that the fatigue life for steel wire varies with different tightening coefficients. For $\eta = 1.4$, fatigue life is approximately 10 years while it is reduced to 7 years after the increase of η

from 1.4 to 1.6. Thus different life time ranges of 0-7 years and 0-10 years should be employed.

With attention placed on seven years, seven time segments from 0-1, 1-2, 2-3, 3-4, 4-5, 5-6 and 6-7 year will be chosen for integration. In Eq. (10), $n=7$ such that the condition $a^1 = a^2 = \dots = a^7 = 1$ is used in Eq. (9). And same can be done to the range of 0-10 years. Ten time segments from 0-1, 1-2, ..., 9-10 year will be chosen for integration. In Eq. (10), $n=10$ such that the condition $a^1 = a^2 = \dots = a^{10} = 1$ is made. These conditions together with the weighted function $\alpha(t)$ in Fig.7 are needed for determining the R-integrals and variances.

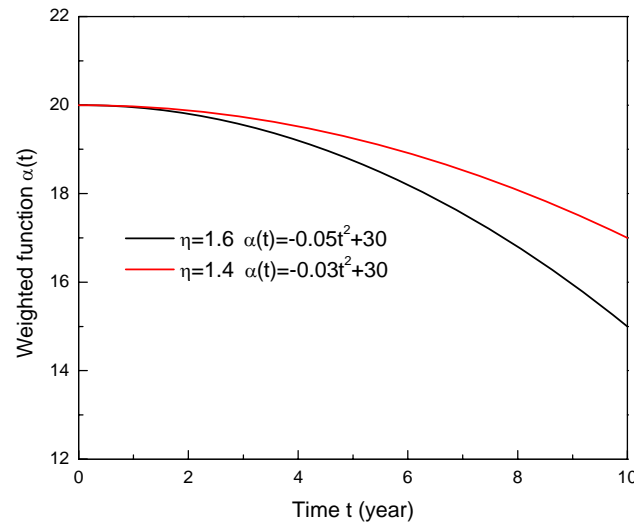


Fig.7 Weighted functions

Choice of weighted function $\alpha(t)$ depends on several factors, It is applied to adjust the time degradation effect of the root function $p(t)$. The decay function can also be seen as a description of material degradation.

5.2.2. R-integrals and variances of crack length

Application of Eqs. (9) and (10) together with the weighted functions in Fig.7, the R-integrals and the corresponding variances for the micro/macro fatigue crack growth of wire in cable no.3 are evaluated. The numerical values can be found in Tables 2-5 inclusive.

Table 2 R-integrals for fatigue crack growth with $\eta = 1.4$

| R_1 | R_2 | R_3 | R_4 | R_5 | R_6 | R_7 | R_8 | R_9 | R_{10} | R_{ave} |
|-------|-------|-------|-------|-------|-------|-------|-------|-------|----------|-----------|
| 23.4 | 31.7 | 42.7 | 57.5 | 77.1 | 103.1 | 137.4 | 182.4 | 241.2 | 317.6 | 121.4 |

Table 3 Variances for fatigue crack growth with $\eta = 1.4$

| ΔR_1 | ΔR_2 | ΔR_3 | ΔR_4 | ΔR_5 | ΔR_6 | ΔR_7 | ΔR_8 | ΔR_9 | ΔR_{10} |
|--------------|--------------|--------------|--------------|--------------|--------------|--------------|--------------|--------------|-----------------|
| 98.0 | 89.8 | 78.7 | 63.9 | 44.3 | 18.3 | 16.0 | 61.0 | 119.8 | 196.2 |

Table 4 R-integrals for fatigue crack growth with $\eta = 1.6$

| R_1 | R_2 | R_3 | R_4 | R_5 | R_6 | R_7 | R_{ave} |
|-------|-------|-------|-------|-------|-------|-------|-----------|
| 25.1 | 38.8 | 59.6 | 91.1 | 138.6 | 209.5 | 314.7 | 125.3 |

Table 5 Variances for fatigue crack growth with $\eta = 1.6$

| ΔR_1 | ΔR_2 | ΔR_3 | ΔR_4 | ΔR_5 | ΔR_6 | ΔR_7 |
|--------------|--------------|--------------|--------------|--------------|--------------|--------------|
| 100.2 | 86.6 | 65.7 | 34.2 | 13.2 | 84.2 | 189.4 |

Depicted in Figs. 8 and 9 are the plots of non-monotonic variations of the data that can be found in Tables 2-5 for crack length. The minima are shown for both of the curves. The curves display the feature of decreasing and then increasing. Distinctive minimum are found to be around 6 years and 4.5 years, respectively. According to the principle of least variance, compare Fig.6 for the reliable portions of the fatigue crack growth. With $\eta = 1.4$, the time range before fast fracture is approximately between 5 and 7 years. Increase of tightening coefficients from 1.4 to 1.6 reduces the reliable portion to be around between 4 and 5 years. It is noticeable that variance for the range of fast fracture deviates tremendously from the average. This means that it is least reliable. The initial stage of crack initiation also possesses substantial deviation from the average. It is, however, relatively difficult for detection at such an early stage. The region of high reliability for the fatigue crack growth can be identified with the span of 5-7 years and 4-5 years, respectively. It should be pointed out that time rates and time intervals also affect the variances in a modest manner. Nevertheless, similar conclusions can be made based on the theory of least variance.

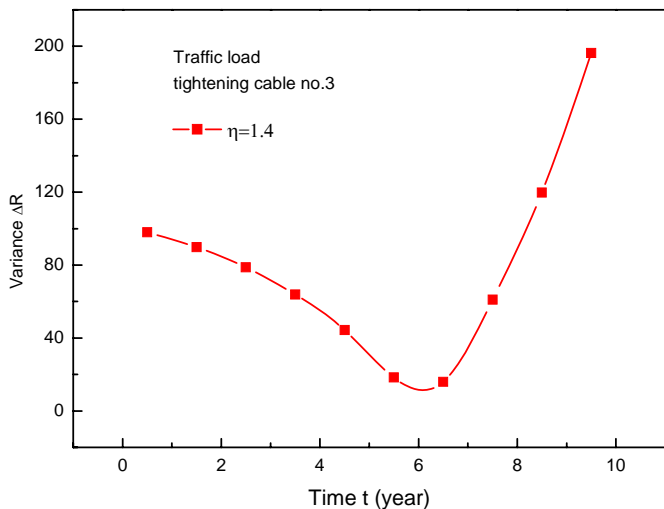


Fig. 8 Variance for crack depth with $\eta = 1.4$

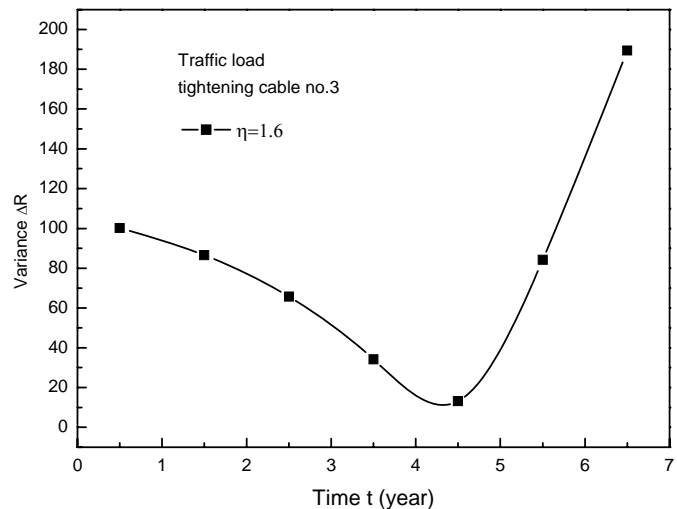


Fig. 9 Variance for crack depth with $\eta = 1.6$

6. Concluding remarks

Long-span bridge cables usually consist of thousands of high strength steel wires that are measured in millimeters. Wire breakages cause the eventual failure of cables. Fatigue degrades the life of wires and cables as well as material aging and stress corrosion. It has become one of the biggest concerns in the maintenances of bridges. Clearly, uncertainty of cable force variation in the operating period can greatly affect the fatigue crack growth behavior. One problem emerges with regard to the inspection of cables. That is, each of the cables is unique on the aspects of loads and configuration. During the operating time, some of the cables may need replacement at a time when other cables of the same bridge may still possess ample remaining life. This poses great challenge for the assessment of reliability of wires and cables.

The theory of least variance offers one of the possible solutions by proposing significant variables including length, velocity, mass and energy. Minimizing the oscillation of R_1, R_2, \dots, R_n has been assumed to be a measure of system reliability. The principle of least variance identifies the

time span to which ΔR_i takes the smallest values. By application of principle of least variance, identification of the most reliable time range to detect micro/macro- fatigue crack growth in the wires of cable has been made possible. The results coincided with the empirical practice in engineering. Over the past decades, the scale of range research interest has been extended to micro, nano and even pico effects. Scale interactive effects for the most part have not been made transparent until the space-time scale ranges were extended to the extremes. These problems have been tentatively explored in the framework of principle of least variance.

With the advent of defect-detecting techniques of 21st century, structural health monitoring system (SHMS) [14] is increasingly installed in the bridges that are newly put on. Collected data are astronomical and interpretation of the field data can be more challenging, since the modern sensors are so accurate that both micro- and macro-effects are often mingled. Theory of least variance together with dual scale modern provides a potential solution for defect detection in SHM. Further applications of theory of least variance to multiscale system and structures are expected. This will be left for future studies.

Acknowledgements

Project supported by SPSFC (the Shanghai Postdoctoral Sustentation Fund, China, Grant No. G200-2R-1238) is appreciated. The author is indebted to Professor George C. Sih for his guidance.

References

- [1] P. C. Paris, The growth of cracks due to variations in load. Ph. D. Dissertation, Department of Mechanics, Lehigh University, 1962.
- [2] G. C. Sih, Simultaneous occurrence of double micro/macro stress singularities for multiscale crack model. *J. Theoret. Appl. Fract. Mech.* 46 (2006) 87-104.
- [3] G. C. Sih, X. S. Tang, Z. X. Li, A. Q. Li, K. K. Tang, Fatigue crack growth behavior of cables and steel wires for the cable-stayed portion of Runyang bridge: Disproportionate loosening and/or tightening of cables. *J. Theoret. Appl. Fract. Mech.* 49(1) (2008) 1-25.
- [4] G. C. Sih, Principle of least variance for dual scale reliability of structural systems. *J. Theoret. Appl. Fract. Mech.* 54 (2010) 137-140.
- [5] G. C. Sih, K. K. Tang, Assurance of reliable time limits in fatigue depending on choice of failure simulation: Energy density versus stress intensity. *J. Theoret. Appl. Fract. Mech.* 64(2) (2010) 117-126.
- [6] G. C. Sih, K. K. Tang, On-off switching of theta-delta brain waves related to falling asleep and awakening. *J. Theoret. Appl. Fract. Mech.* (2013) <http://dx.doi.org/10.1016/j.tafmec.2013.03.001>
- [7] G. C. Sih, K. K. Tang, Sustainable time and stability of hippocampal and cortical EEG theta waves. *J. Theoret. Appl. Fract. Mech.* (2013), dx.doi.org/10.1016/j.tafmec.2013.01.001
- [8] G. C. Sih, K. K. Tang, Sustainable reliability of brain rhythms modeled as sinusoidal waves with frequency-amplitude trade-off. *J. Theoret. Appl. Fract. Mech.* 61 (2012) 21-32.
- [9] Q. B. Ou, Construction of Runyang Bridge: Cable-stayed Portion. China Communications Press, Beijing, 2005.
- [10] S. Y. Wang, Z. J. Dang. Research on heavy-load high fatigue stress amplitude cable and anchorage of cable-stayed bridge. *J. of Bridge Construction*, 3(2002) 14-16.(in Chinese)
- [11] Editorial Board, Practical Handbook of Engineering Materials. Chinese Standard Press, Beijing, 2002.
- [12] G. C. Sih, Crack tip mechanics based on progressive damage of arrow: hierarchy of singularities and multiscale segments. *J. Theoret. Appl. Fract. Mech.* 51(1) (2009) 11-32.
- [13] G. C. Sih, Ideomechanics of transitory and dissipative systems associated with length, velocity, mass and energy. *J. Theoret. Appl. Fract. Mech.* 51(3) (2009) 149-160.
- [14] J. P. Ou, H. Li, Structural health monitoring in mainland China: review and future trends. *Struct. Health Monit.* 9(3)(2010) 219-231.